Journal of Energy Storage 46 (2022) 103807

Contents lists available at ScienceDirect

Journal of Energy Storage

journal homepage: www.elsevier.com/locate/est

Techno-economic analysis of a nuclear-wind hybrid system with hydrogen storage

Tian Zhang

College of Nuclear Science and Technology, Harbin Engineering University, Harbin, China

ARTICLE INFO

Keywords:
Genetic algorithm
Nuclear-renewable hybrid system
Optimization
System analysis
Techno-economic simulation

ABSTRACT

Climate change and increasing electricity demand have changed the electricity generation structure to include more renewable energy. To keep the global temperature increment within 2 °C, the fraction of renewable energy in the energy mix will continuously increase. High penetration of wind and solar energy challenges the electricity grid as they are not dispatchable. Hybrid energy systems with energy storage have the opportunity to meet the challenge due to their stability and flexibility in energy dispatching. However, their performances and economics remain questionable and quantitative analyzes are needed. In this work, Hybrid Nuclear-Renewable Tool (HyNuRT) code is developed to analyze the technical and economic performance of a hybrid nuclear-wind system with hydrogen storage. In the code, technical models of wind turbines, nuclear units, and hydrogen production and storage units are developed and coupled to economical evaluation models. The economic model considered features of a small modular reactor which is more suitable to couple with renewable energy due to its lower power output and modular fabrication. The novelty of this method is to estimate system performance of typical months of the year with stochastic real-time data and predict system economic value including the construction phase. This method is computational time-saving and makes optimization possible in a relatively short time. The work analyzed the techno-economic performances of conservative and balanced cases to evaluate their performances and economic values by real grid demand data. Results show balanced case can increase the internal return rate by 2.1% with missing only limited peak demand. Comparison of hybrid nuclear-wind systems with and without hydrogen storage show that with assumptions in this work, hydrogen storage shows its advantage on both to meet the grid demand and increase the economic return by 1% while not strongly impacting the cash flow. The results show hybrid system with hydrogen storage can enhance both the system performance and the economic value under proper configuration.

1. Introduction

Electricity is essential for the modern society and the economy. In the past twenty years, global electricity demand has increased by over 70% due to the increasing demands in developing countries like China and India [1]. By predictions, up to the year 2040, the electricity demand will keep increasing with a rate of over 2% [1,2]. Meanwhile, global warming challenges the global electricity market. Greenhouse gas emissions need to be controlled to meet the target of keeping temperature increment under 2 °C. The division of "more energy" and "less carbon" promotes the integration of renewable energy, particularly wind and solar energy, into electricity generations. In the year 2017, the share of wind and solar was about 6% while in the year 2000 the figure was merely 0.2% [2]. This figure increased to 9.5% in 2020 [3] and according to prediction, their share will be 22% in 2030, 30% in 2040, and 40% in 2050 [4,5].

In contrast to the advantage of supplying carbon-free electricity, wind and solar energies have their drawbacks. As their power production depends on the weather, it is not dispatchable. Under high renewable penetration, such property challenges the grid when weather is not favorable for wind and solar energy production.

To cope with the future energy mix, a possible plan is to include hybrid energy systems in electricity generation. A hybrid energy system

Abbreviation: COA, Code of Account; CF, Cash Flow; DOE, U.S. Department of Energy; EEDB, Energy Economic Data Base; FOAK, First of a Kind; HES, Hybrid Energy System; HNRS, Hybrid Nuclear Renewable System; HNWS, Hybrid Nuclear Wind System; IDC, Interest During Construction; IRR, Internal Return Rate; LCOE, Levelized Cost of Energy; LR, Large Reactor; NOAK, Nth of a Kind; NPP, Nuclear Power Plant; NPV, Net Present Value; OCC, Overnight Capital Cost; PEM, Proton Exchange Membrane; PWR, Pressurized Water Reactor; SMR, Small Modular Reactor.

E-mail address: tian.zhang@hrbeu.edu.cn.

https://doi.org/10.1016/j.est.2021.103807
Received 26 September 2021; Received in revised form 8 December 2021; Accepted 9 December 2021
Available online 24 December 2021

Nonmolecular

A	area (mm)
C_p	wind power efficiency coefficient
D	wind turbine diameter (m)
E_{oc}	open circuit voltage (V)
F	Faraday constant 96485.3329 ($C\ mol^{-1}$)
I	Current (A)
i_0	exchange current density (A/cm^2)
n	number of units
$\dot{n}_{H2}$	hydrogen production rate (mol/s)
P	output power (MW)
T	temperature (°C)
V_{cell}	cell voltage (V)
v	velocity (m/s)

Greek letters

α	charge transfer coefficient
η_{act}	activation overvoltage (V)
η_{ohm}	ohmic overvoltage (V)
ρ	Density (kg/m^3)
σ_m	conductivity of the PEM ($W/m.K$)

Subscript

an	anode
cat	cathode
nu	nuclear
tur	turbine
w	wind

(HES) combines two or more forms of energy generation, storage, or end-use technologies and can deliver a boatload of benefits compared with a single energy system [6]. Normally it requires a base-load source and variable energy such as wind or solar. Nuclear energy, as a sustainable and reliable low-carbon electricity source, is an option for the base-load source in a hybrid energy system. The large capital cost and low fuel cost of nuclear energy require a nuclear power plant running at high capacity, which is one of the advantages of HES [7]. Hence, Hybrid Nuclear-Renewable Systems (HNRS) are considered as one form of future energy systems. Meanwhile, besides dynamical carbon-free electricity, hybrid nuclear-renewable systems can co-produce products like heat and/or chemical energy which can meet the demand in the industrial and transport sectors [8].

Different ways of coupling and co-generation products are possible for HNRSs, such as producing biofuel by thermal coupling with biomass or heat with concentrated solar power [7]. In this work, concentrations are put on the Hybrid Nuclear-Wind System (HNWS).

Numbers of studies have been performed on HESs and HNWSs. Mazzeo et al. [9] reviewed 550 articles studying hybrid photovoltaic-wind systems in the past 25 years, they found out that most studies focus on installing such systems in warm or temperature regions, and the power output of such systems is relatively low, more suitable to the residential region rather than industrial scale. Wang et al. [10] designed and conducted an economic analysis of a novel hybrid nuclear-solar system, which coupled a 200 MW nuclear power plant to a solar tower. The system produces fresh water in the meantime. The found out for such a system, the levelized cost of electricity is down to 51.7 $/MWh, and the cost for freshwater production is cheaper than a coal power plant driven desalination plant. Suman [11] reviewed challenges of renewable energy and nuclear energy, and type of coupling, interconnections, benefits, and challenges faced, and qualitatively stated the opportunities of HNRS in the future. Pinsky et al. [12] reviewed hydrogen production technologies that can be used for nuclear hybrid energy systems and discussed the most suitable technology for different nuclear reactor designs. Baker et al. [13] conducted multi-objective optimization with RAVEN code on an HNWS with battery storage and desalination plant with wind volatility. They found that volatility exponentially increases the cost of the energy system and battery storage is valuable in such systems. Epiney et al. [14] proposed a new framework of economic analysis based on Modelica language and RAVEN code. Their study shows that under the condition of stochastic wind speed and grid demand, HNRSs can be economically favorable with suitable industrial processes. Ruth et al. [15] performed techno-economic analyzes for HNWSs that co-generate different industrial products in different regions of the U.S. They draw a series of conclusions on the co-generating industrial processes with different electricity price and co-product price models. They pointed out a maximum number of industrial processes operations usually maximize profitability in a year. They also found a lower capital cost industrial process can increase the switching flexibility which increases the number of profitable situations. Ross and Bindra [16] developed a continuous-time stochastic model for HNWS with energy storage and analyzed the required storage type and operation mode. They found out that flexible operation of nuclear power can reduce the storage requirement and compared with Li-ion and pumped-hydroelectric, thermal storage has the lowest size and highest utilization factor. Arent et al. [17] reported the perspective of a multi-input, multi-output HES, they consider tightly coupled HES as a key attribution to the future energy system, however, new modeling capabilities are needed to meet the energy demand constraints.

The perspective of HNWS looks attractive. However, most studies either perform technical analysis or economic analysis with uncertainty, simulations with dynamic power production from mechanism level modeling are not sufficient. Moreover, coupling to hydrogen as energy storage is not sufficiently studied, quantitative analyzes are needed to further understand whether HNWS with hydrogen storage fits the dynamic demands of the grid. Besides, under the trends of deploying small modular reactors, features of small modular reactors are rarely considered in current economic analyzes, particularly the influences of the number of modules to the system economics are not well conducted. These features influence both capital cost and deployment schedule as well as the optimized system size.

In this work, a method is developed trying to include mechanical level dynamic simulation together with system size optimization considering small modular reactor deployment and economical features. By this method, the economics of an HNWS can be evaluated based on typical real-time system performances. In Section 2, the generic structure of an HNWS with hydrogen storage and its advantage are introduced. Section 3 gives descriptions of technical models and economic models implanted in this work. Results and discussion of analyzed cases are given in Section 4. Conclusions are summarized in Section 5 as well as the future development.

2. Hybrid nuclear-wind system with hydrogen production

Besides the properties being mentioned in the introduction section, Small Module Reactor (SMR) today brings new solutions to Nuclear Power Plant (NPP) deployment. SMR's smaller size and modular design offer flexibility to NPP capacity installation. Furthermore, the unique economic features of SMR designs make the capital cost and the cash flow more favorable to investors than traditional commercial Large Reactors (LRs) [18].

The coupling in an HNWS is achieved by the electrical method with hydrogen as the intermediate storage media. Hydrogen is also being

Table 1
Three Approaches of Water Electrolysis [20].

	Alkaline electrolysis	Membrane electrolysis	Solid oxide electrolysis
Temp. Range	40–90 °C	20–100 °C	700–1000 ℃
Cathodic Reaction	$2H_2O$ + $2e^- \leftrightharpoons H_2 + 2OH^-$	$2H^+ + 2e^- \leftrightharpoons H_2$	H_2O + $2e^- \leftrightharpoons H_2 + O^{2-}$
Charge Carrier	OH^-	H^+	O^{2-}
Anodic Reaction	40–90 °C	20–100 °C	$O^{2-} \leftrightharpoons 1/2O_2 + 2e^-$

treated as a co-product of the system. The hydrogen industry is well established and expected to grow significantly [19]. As a co-product, hydrogen has a good market value.

Hydrogen is widely demanded in chemical sectors and future transport sectors, it can help the HNWS gain profits when there is too much excessive electricity. Various ways can produce hydrogen, most commonly used today is by steam-methane reforming, which is fossil-fuel based [19]. Water electrolysis, as a carbon-free hydrogen production technology, can produce high purity hydrogen and be used as energy storage and co-production for the hybrid energy system. Energy conversation in water electrolysis is between electricity and hydrogen, in one way or the other. The basic equation of the reaction is written as Eq. (1):

$$H_2O + Electricity \rightleftharpoons H_2 + \frac{1}{2}O_2 \tag{1}$$

Three approaches are possible for water electrolysis: alkaline electrolysis, membrane electrolysis, and solid oxide electrolysis, as listed in Table 1. Among these technologies, Proton Exchange Membrane (PEM) has the advantages of compact design, high current density, high efficiency, and fast response [21]. Thus, it is favorable for hybrid energy systems. The fast response of PEM units suits the dynamics of renewable energy, which may change dramatically due to the change of weather conditions. The relatively low operating temperature of PEM makes it also suits to the operation range of light water SMRs discussed in this work [12].

The layout of a typical HNWS with hydrogen storage is shown in Fig. 1. As discussed in this section, the basic structure of an HNWS: an NPP, a wind farm, and clusters of PEMs for energy storage. By off-grid dispatch, excessive electricity can store in the form of hydrogen at low demand hours, while the stored hydrogen can produce electricity to meet the peak time demand. Stored hydrogen can also be sold on the market to meet the demand of various end-users and improve the economics of the HNWS.

3. Modeling approach

Techno-economic analysis of an HNWS requires modeling of both technical and economic aspects in component and system scales. The modeling strategy in this work is to divide the model into technical analysis model and economic analysis model. These two models are coupled with each other via data exchange and interpolation. Moreover, optimization models are implemented to support the system-level techno-economic analysis.

Hybrid Nuclear-Renewable Tools (HyNuRT) code [22] is developed to perform the analysis. HyNuRT code is developed under the GPLv3 license. It is written in python3 with a modular design of technical modeling, economic modeling, and coupling interface. In the following sections, models implemented in HyNuRT code are described.

3.1. Technical models

For technical modeling, the code includes the models of the wind energy model, the nuclear power model, the PEM converter model, and the storage model as well as the off-grid dispatch model.

3.1.1. Wind energy

The wind energy model has two levels: wind turbine level and wind farm level. The wind turbine model is the base of wind energy modeling.

For a given wind speed v, the total kinetic power of the wind P_w can be calculated by Eq. (2) [23]:

$$P_w = \frac{1}{2}\rho_{air}\frac{\pi D^2}{4}v^3 \tag{2}$$

where ρ_{air} is the density of air and D is the rotor diameter. Not all kinetic energy of wind convert to power, the harvest power of wind turbine is constraint by the power efficiency coefficient C_p, which can be written as Eq. (3) [23]:

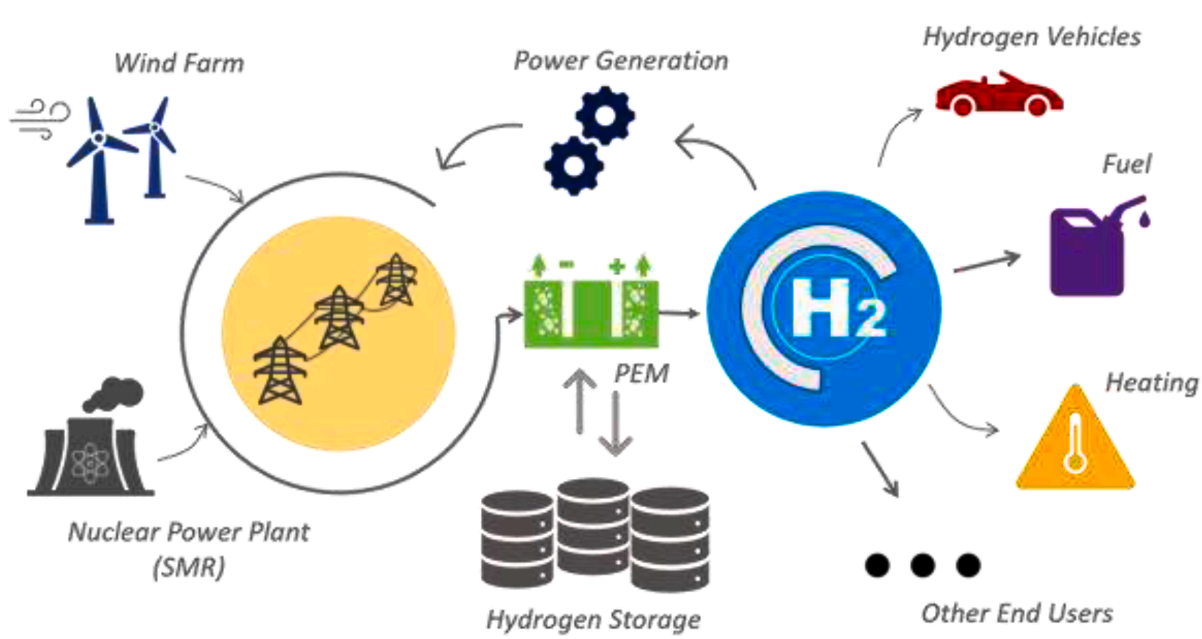

Fig. 1. Layout of a Hybrid Nuclear-Wind System with Hydrogen Storage.

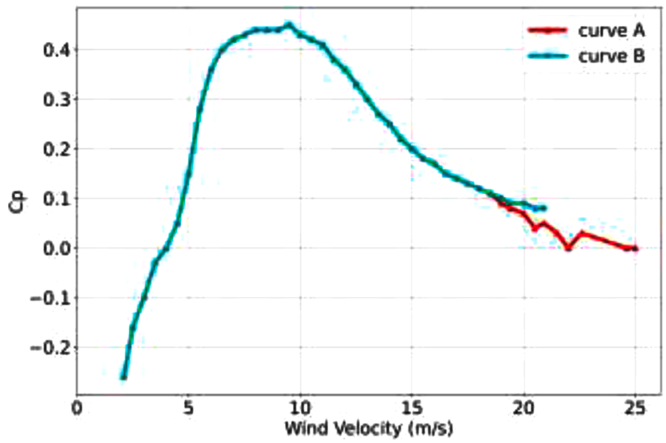

Fig. 2. Cp curves from IEC 61,400–12–1[18].

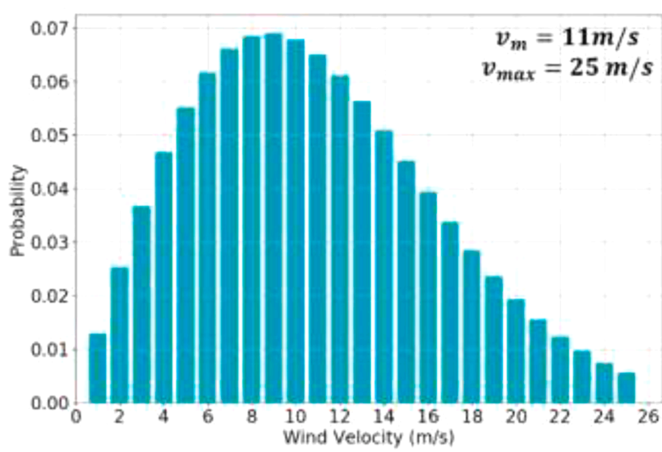

Fig. 3. Rayleigh distributed wind velocity for $v_{ave} = 11\ m/s$ and $v_{max} = 25\ m\ /s$ with 25 intervals.

$$P_{harv} = C_p P_w \tag{3}$$

As wind turbine can only produce power in the range between 0 and designed maximum power output P_{max}, the power generated by the turbine P_{tur} is defined as:

$$P_{tur} = \max(0, \min(P_{harv}, P_{max})) \tag{4}$$

The power efficiency coefficient C_p is a function of wind velocity v. In the code, two default C_p curves are set, as plotted in Fig. 2. Both curves are taken from IEC 61,400-12-1 [24], however, users can also input their curves, too.

The model of the wind farm is a simplified model. The reduction of wind energy is currently not considered in the current model. The output power of a wind farm is modeled as the product of wind turbine energy and the number of units functioning, n_{tur}, as described in the following equation:

$$P_{farm} = P_{tur} n_{tur} \tag{5}$$

The energy conversation is based on the wind velocity. In the HyNuRT code, a module is implemented to generate time-dependent wind velocity from statistical wind data. In the model, the wind velocity distribution is calculated by Rayleigh distribution, which is expressed as formula (6) [25]:

$$\mathrm{h(v_i)} = \frac{\pi}{2}\frac{\mathrm{v_i^2}}{\mathrm{v_m^2}}\exp\left(-\frac{\pi}{4}\frac{\mathrm{v_i^2}}{\mathrm{v_m^2}}\right) \tag{6}$$

where i is the index of the interval, v_m is the average wind velocity.

An example of Rayleigh distribution is shown in Fig. 3. In the example, wind average velocity v_{ave} is set to be 11 m/s while the maximum velocity v_{max}. of 25 m/s is set. The velocity is distributed in 25 intervals.

Time-dependent wind velocity is calculated by random numbers. In each time-step, a random number $\xi \in [0, 1]$ is generated, by comparing ξ and the cumulative Rayleigh distribution, a wind velocity is generated.

Through these models, time-dependent wind farm output power is calculated according to different wind conditions and power coefficient curves.

3.1.2. Nuclear power

The model of NPP is relatively simple. Each unit of a nuclear reactor is considered tbe a constant power generator. To guarantee the NPP works under high capacity, no load-following it set. The output power P_{nu} of the NPP is calculated as the product of designed power of a unit, P_{unit}, and number units, n_{unit}, as following described in the following formula:

$$P_{nu} = P_{unit} n_{unit} \tag{7}$$

3.1.3. Hydrogen converter and storage

The production and consumption of hydrogen are carried out in the same mechanism [21]. Thus, the process can be simulated by a reversible model. Moreover, the storage of hydrogen also influent the performance of the HNWS, a simple model calculates the dynamics of the storage is applied.

The basic unit of the hydrogen conversation is a PEM unit. A model is built to simulate the quasi-steady behavior of a PEM unit. As PEM units have response time at the level of milliseconds [26], such an approach is considered reasonable for a dynamic simulation with minimum time-steps in minutes scale.

The convert rate of hydrogen is given by Faraday's law [27]:

$$\dot{n}_{H2} = \frac{I}{2F} \tag{8}$$

where F is the Faraday constant, I is the current between the anode and the cathode.

In PEM units, the cell current is related to the cell voltage. The cell voltage can be modeled as the sum of open-circuit voltage E_{oc}, activation overvoltage η_{act}, and ohmic overvoltage η_{ohm}:

$$V_{cell} = E_{oc} + \eta_{act} + \eta_{ohm} \tag{9}$$

In Eq. (9), the open-circuit voltage is calculated using the Nernst equation taking into account the effects of temperature and species concentration [28]:

$$E_{oc} = E^0_{rev} + \frac{RT}{nF}\left(\frac{P_{H2}P_{O2}^{\frac{1}{2}}}{P_{H_2O}}\right) \tag{10}$$

where:

$$E^0_{rev} = 1.229 - 0.0009(T - 298.0) \tag{11}$$

and T is the operating temperature, P is the pressure of different species.

The activation overvoltage is described by the Butler-Volmer equation for both anode and cathode [28]:

$$\eta_{an} = \frac{RT}{\alpha_{an}F}\operatorname{arcsinh}\left(\frac{I}{2i_{0,an}}\right) \tag{12}$$

$$\eta_{cat} = \frac{RT}{\alpha_{cat}F}\operatorname{arcsinh}\left(\frac{I}{2i_{0,cat}}\right)$$

$$\eta_{act} = \eta_{an} + \eta_{cat}$$

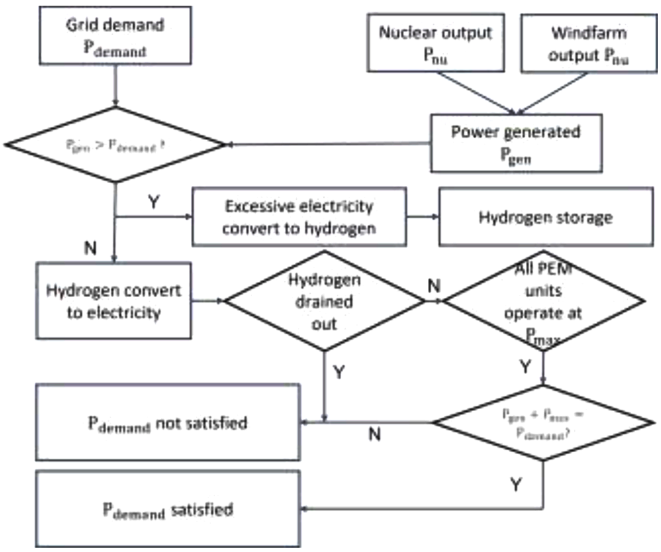

Fig. 4. Flowchart of the off-grid dispatch model.

in which R is the ideal gas constant, α is the charge transfer coefficient, and i_0 is the exchange current density at the electrodes.

The ohmic overvoltage is due to the resistance in the cell, mainly due to the membrane, which can be modeled by Eq. (13) [28]:

$$\eta_{ohm} = \frac{\delta_m I}{A\sigma_m} \tag{13}$$

where δ_m and A is the thickness and the area of the membrane, respectively. σ_m is the conductivity of the PEM, which is given by [29]:

$$\sigma_m = (0.005139\lambda - 0.00326) \exp\left[1268\left(\frac{1}{303} - \frac{1}{T}\right)\right] \tag{14}$$

where λ is the water uptake coefficient of the membrane. In the current model, the value of λ is assumed to be 20 [28].

Combining Eq. (8) to Eq. (14), the production or consumption rate of hydrogen is modeled. A simple model of hydrogen storage is also developed to account for the amount of hydrogen that can be used for dynamic load following. The model assumes zero storage at the beginning of the simulation. In each time-step, produced or consumed hydrogen is added to or drained from the storage, unless the storage is drained to empty. However, it should be noted, in the current model, no up-limit of storage is set at the moment. This increases the possibility in the later optimization model.

3.1.4. Off-grid dispatch

One target of implementing HNWS is to meet the dynamic demand of grid load. To achieve the target, off-grid dispatch between generators (wind farm, NPP) and PEM stacks is performed. The electricity dispatching model has the priority to satisfy the demand of the grid, which is an input for the code. The flowchart of the dispatch process is shown in Fig. 4. In each time step, a comparison between the grid demand P_{demand} and the total generated electricity P_{gen} is conducted. If $P_{gen} > P_{demand}$, excessive electricity will be dispatched to PEM stacks and converted electricity to hydrogen and stored. On the other hand, if $P_{gen} < P_{demand}$, hydrogen being stored is consumed to produce the gap power ΔP. However, under two conditions, the grid demand is not satisfied: (a). hydrogen storage is drained to empty; (b). all PEM cells have been working at their maximum designed power. Under these two conditions, PEM stacks output the maximum power they can generate.

As PEM cell stacks for producing hydrogen have minimum operation power, when $P_{gen} > P_{demand}$, excessive power is averaged to all PEM cells. If the average cell power is lower than the minimum PEM operating power, some of the PEM cell units will be shut down to keep the rest of the PEM cells operating at the minimum required power.

3.2. Economic models

On the aspect of economic evaluation, the code contains models of nuclear, wind, and PEM economics, respectively. The code can also calculate system economic parameters, such as Cash Flow (CF), Net Present Value (NPV), and Internal Return Rate (IRR). As HNWS is not built in a short period, an automatic deployment schedule model is developed for the HyNuRT code.

3.2.1. System economics

The evaluation of the economics of HNWS is based on four parameters: the CF, the NPV, the IRR, and the Levelized Cost of Electricity (LCOE). These four parameters can effectively describe the system's cost and expected economic return over the system's lifetime.

Cash flow is an indicator to show how much cash one company is holding in hand. It is calculated by the sum of annual net cash, which is the difference between the profits and the costs. In an HNWS, profits come from selling electricity and hydrogen, costs are the cost of each component in the system, which is presented in the following sections.

The NPV is the discounted value of all annual cash flows, NPV of an N year project with a discount rate d_r is calculated by the following equation [18]:

$$NPV = \sum_n \frac{CF_y}{(1+d_r)^y} \tag{15}$$

If NPV is larger than zero, the project is considered worth investing, otherwise, it is not [30].

The IRR describes the return on investment over the lifetime, it is determined by iteration on the marginal NPV [18]. When the IRR of a project is larger than the discount rate, the project is profitable and worth to invest.

LCOE represents the lifetime energy cost of a system. It is an indicator that determines the cost of electricity per MWh. The LCOE of the HNWS is given by:

$$LCOE = \frac{\sum_n Discounted\ CF}{\sum_n Discounted\ Electricity} \tag{16}$$

In the current model, the avenue from hydrogen is not included while calculating the LCOE.

3.2.2. Nuclear economics

The cost of an NPP can be broken into two parts: the capital cost and the operational cost. In the economic model of the HyNuRT code, the model of capital cost and operational cost are implemented, respectively.

The capital cost of an NPP is again broken into the Overnight Capital Cost (OCC) and the Interest During Construction (IDC). The IDC is related to the OCC and the construction time of the NPP. Hence, the estimation of OCC decides the amount of capital cost.

The OCC of an NPP depends on the installed capacity. An equation is suggested to estimate the effect of changes on the capacity [31]:

$$Cost(P) = Cost(P_{base})\left(\frac{P}{P_{base}}\right)^n \tag{17}$$

where P is the power of the target unit, P_{base} is the power of the reference plant, and n is the scaling factor. In the HyNuRT code, n is default set to be 0.51 [32]. Users can apply other values, too.

In the HyNuRT code, the reference cost is based on the Energy Economic Data Base (EEDB) from the U.S. Department of Energy (DOE)

Table 2
Comparison of nuclear cost between HyNuRT and references [32,37,38].

Type	Power (MW)/lifetime (year)	OM ($/MWh)	Fuel ($/MWh)	DCMS ($/MWh)	Reference OCC (/kW)	Reference LCOE (/MWh)	Model OCC (/kW)	Model LCOE (/MWh)
EPR (France) [32]	1600/60	16	9.3	0.16	$3860	$56.4	$3320	$53.3
Advanced Gen.III (USA) [32]	1350/60	12.8	9.3	0.16	$3382	$48.7	$3609	$52.5
Nuscale (FOAK) [37]	47.5 × 12/60	36.2		0.16	$5078	$65.0	$5250	$75.5
Nuscale (NOAK) [38]	57×12/60	36.2		0.16	$3600	$65.0	$3980	$66.0

* EPR and Advanced Gen. III costs are in 2009 dollar
* Nuscale (FOAK) cost is in 2015 dollar
* Nuscale (NOAK) cost is in 2018 dollar
* **Note: Power Output is changed for NuScale SMR unit as the design updated**

[33]. The EEDB is a Code of Accounts (COA) system that utilizes a common cost when assessing the capital cost of NPPs across designs and time [34].

The EEDB adopted PWR12 as the reference plant, which is a four-loop Pressurized Water Reactor (PWR) of 1144 MW electrical power [33]. Many PWR12 type NPPs were constructed during the 1970s and the 1980s. Hence, experiences were gained and quite some data were collected. These data were grouped into median and better experience in terms of COA to help to estimate the cost of NPP [33]. These data are recorded in 1987 dollars. While implementing in the HyNuRT code, with the python cpi module [35], data can be interpolated to recent years. With the EEDB, the direct cost and the indirect cost of an NPP can be estimated.

As in the framework of the currently developed method, the NPP is deployed in the form of SMRs, economic features of SMR are included in the model. These features can either increase the capital cost or reduce it in most cases.

The learning reduction factor is one feature of SMR economics. It can be divided into two parts: plant configuration and technological maturity [30]. Plant configuration learning is due to a better construction work organization, learning effect, or other factors [32]. However, the First-of-a-Kind (FOAK) will cause extra cost while the Nth-of-a-Kind (NOAK) will not. For n SMR units, the plant configuration factor can be summarized in the following equation [32]:

$$f_{con} = \sum_{n} f_i \tag{18}$$

where f_i stands for the plant configuration factor for the *ith* unit, and f_i is given by Eq. (19) [32]:

$$f_i = \begin{cases} 1 + x \ if \ FOAK, \ 1 \ if \ NOAK \\ \dfrac{y \ or \ z}{(1+k)^{i-2}} \ y \ for \ even, \ z \ for \ odd \end{cases} \tag{19}$$

In Eq. (19), four parameters x, y, z, k has the following meaning and recommend ranges [32]:

- x is FOAK extra cost parameter, 15–55%
- y is related to gain in building a pair of units, 74–85%
- z is related to gain in building two pairs of units, 82–95%
- k is industrial productivity coefficient, 0–2%

Technology maturity is another effect that influences the cost of SMR. This factor is due to from FOAK to NOAK, the technology is getting mature. Technology maturity factor is given by [30]:

$$f_{learn} = (1+x) P_{NPP}^{-\frac{\log(1-R)}{\log(2)}} \tag{20}$$

where P_{NPP} is the electrical power of an NPP, and R is the learning rate. R is normally in the range between 1% to 6%, and according to studies, a learning rate of 3 to 4.5% is normally taken [30].

Besides learning, co-siting of SMR units improves the economy, too. Co-citing allows SMR units to share parts of components and reduces the cost. This reduction is related to the indirect cost of the SMR unit F_{ind}, which is calculated by Eq. (17). The co-siting factor is calculated by [36]:

$$f_{co} = \frac{1 + (n-1)(1 - F_{ind})}{n} \tag{21}$$

One more factor that affects the economics of SMR is the modular design. Modular design allows SMR to be fabricated in a factory. Its effect is related to the electrical power of the SMR unit and is given by the following equation [30]:

$$f_{mod} = \begin{cases} 0.6, \ P_{unit} \le 35MW_e \\ 4 * 10^{10} P_{unit}^3 - 10^{-6} P_{unit}^2 \\ +0.0012 P_{unit} + 0.581, \\ 35 \ MW_e < P_{unit} < 600 \ MW_e \\ 1, P_{unit} \ge 600 \ MW_e \end{cases} \tag{22}$$

To summarize, the OCC of an NPP of n SMR units is calculated by:

$$OCC = OCC_{scale} f_{con} f_{learn} f_{co} f_{mod} \tag{23}$$

As an NPP is not built in a day, interests are produced and need to be paid during the construction, which is referred to be IDC. In the current model, IDC in N construction years with interest rate r is considered equally distributed, and can be estimated by the following equation [30]:

$$IDC = \frac{N}{2} \left[\frac{OCC}{N} (1+r)^{N-1} - \frac{OCC}{N} \right] \tag{24}$$

Operational cost consists of operation and maintenance (OM) cost, fuel cost, and decommissioning (DCMS in Table 2) cost. In the model, all these costs are considered as a function of the utilization factor f_{uti}, and given by:

$$Cost_i = Cost_{MWh}^i * f_{uti} \tag{25}$$

where i stands for cost of OM, fuel, or decommissioning in MWh.

Verification of the model is conducted by comparing the model with reference cases of different reactor designs and output powers. In the calculation, while including the SMR economic features, following values in Eq. (19) and (20) are applied: $x = 0.15$, $y = 0.74$, $z = 0.82$, $k = 0.02$, learning rate $R = 0.04$. To calculate the operating cost of the NPP, the utilization factor of 0.85 is used. In all the calculations, dollars of the year of the reference case are taken.

The results are listed and summarized in Table 2. In this table, OCC per kW and LCOE of two larger reactors and the NuScale SMR (FOAK and NOAK) are calculated and compared with reference calculations. In

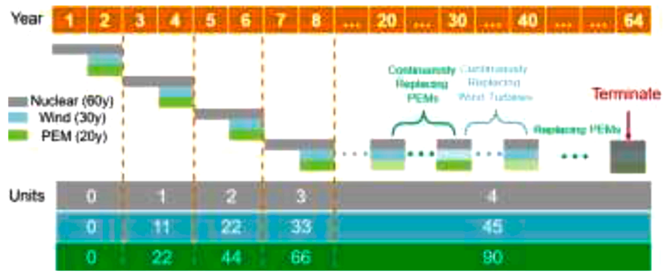

Fig. 5. Example of the default construction and replacement schedule.

Table 3
Example schedule input data.

Component	num	cons	Lifetime
SMR	4	2	60
Wind Turbine	45	1	30
PEM units	90	1	20

all four cases, calculated results are reasonably agreed to the reference values from OECD NEA studies and the vendor's estimations [32,37,38]. Results from large reactors show the correctness of the scaling effect, and SMR cases indicate the economic feature of SMRs are implemented correctly. These comparisons show that the nuclear economic model of the HyNuRT code gives a reasonable estimation on both OCC per kW and LCOE of an NPP.

3.2.3. Wind and hydrogen economics

The economic model of the wind farm is split into capital cost and operational cost, too. However, the capital cost is treated as an input in unit dollar/kW, which users must define the value themselves. Operational cost is broken up into OM cost and decommissioning cost. This is due to no fuel being needed in wind farms. In the current model, operational cost is a function of intermittence factor and in dollar per MWh.

The hydrogen economic model is similar to the wind farm economic model. The model also breaks up the cost into capital cost and operational cost. The operational cost in the current model is accounted as a ratio of the capital cost. In the current model, the cost of hydrogen storage has not yet been implemented.

3.2.4. Deployment and replace schedule

One advantage of deploying SMRs or including SMRs in a hybrid system is that the capital cost is not required upfront [30]. Such a feature flattens the cash flow and reduces the burden on the vendor. However, the feature challenges the deployment strategy of units in an HNWS. Meanwhile, as nuclear reactors normally have the longest lifetime, wind farms and PEM units need to be replaced during the lifetime of an HNWS, which are extra capital costs.

In the HyNuRT code, users can write their deployment schedules. Besides, a default schedule of deployment and replacement is implemented in the code. In the default schedule, the deployment is performed in batch according to the number of SMR units. In the schedule, an HNWS is divided into n batches for construction, where n is the number of SMR units. In each batch, besides an SMR unit, n_{wind}/n wind turbines and n_{h2}/n PEM units are deployed, where n_{wind} and n_{h2} are the numbers of wind turbines and PEM units, respectively. While constructing each batch, all units in the batch will start operation in the same year. Furthermore, when wind turbines or PEM units in a batch achieve their lifetime limit, they will be replaced by the same year.

An example of the default deployment and replacement schedule is given in Fig. 5. Inputs like the number of units (num), construction durations (cons) in the unit year, and lifetime in the unit year are listed in Table 3. As there are four SMR units to be deployed, the construction is divided into four batches: the first three batches include an SMR unit, 11 wind turbines, and 22 PEM units, and the rest units are constructed in the last batch. The duration of construction of each batch is two years. When wind turbines and PEM units reach their life limit, if SMR units will continue to operate, new wind and PEM units will be deployed. This is an example showing how the default schedule works.

3.3. Techno-economic coupling

In the techno-economic analysis of an HNWS, coupling between the technical model and the economic model is a necessary step. This is due to the current technical model being a quasi-steady-state model that simulates a period that normally a few hours or days, in some cases, months. On the other hand, economic analysis is based on annual data, it calculates parameters on a system lifetime scale. Moreover, the

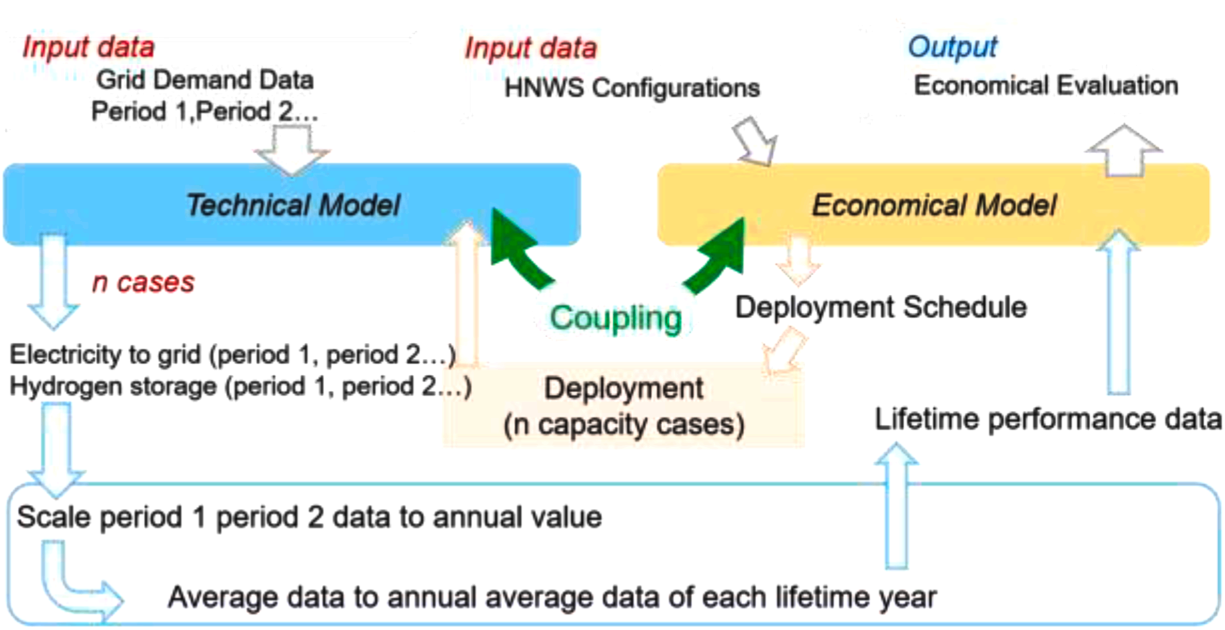

Fig. 6. Overview of the coupling scheme of technical model and economic model in the HyNuRT code.

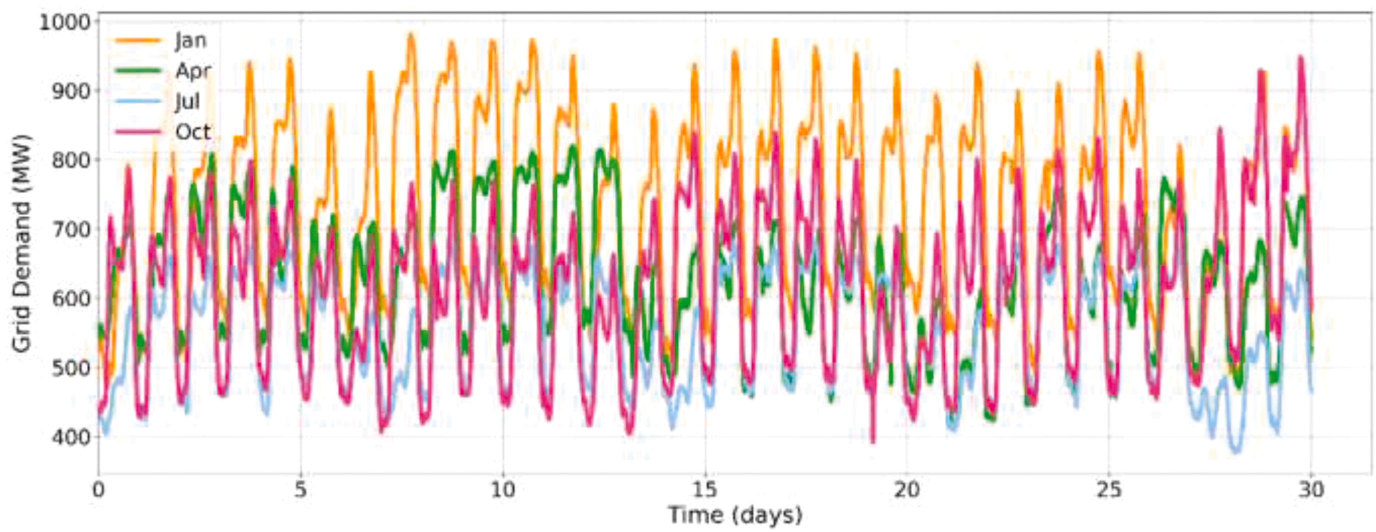

Fig. 7. 2% of UK 2018 grid demand data in Jan. Apr. Jul. and Oct.

deployment schedule is needed by the performance model to determine the number of cases to evaluate. Hence, a coupling interface is developed to match data in both aspects.

Fig. 6 shows the coupled calculation scheme. At the beginning of the calculation, the coupling interface collects the deployment schedule from the economic model. For each batch, a technical calculation is conducted to further estimate the avenues of the HNWS in the following construction years. For each technical calculation, grid demand data of one or more periods are read as input for calculation, data like electricity sent to the grid, accumulated hydrogen storage, etc. are calculated and scaled to annual data and send to the economic model for evaluation.

3.4. Configuration optimization

An HNWS includes different components with a different number of units. Not all the commitment configurations can both meet the grid demand and gain economic profits. An optimized configuration can increase the system investment return without losing too much to meet the grid demand.

The optimization model implemented in the HyNuRT code uses the genetic algorithm to optimize the unit number of each component in the HNWS. The primary target of this work is to evaluate whether an HNWS can gain a high economic return while meeting the grid demand as much as possible. Hence, the IRR and the grid fitting ability are selected as the optimization constraints.

The flowchart of the algorithm is shown in Fig. 7. The algorithm starts with an input configuration, and it generates a batch of n configurations randomly in a pre-defined range which is called populations. Simulation is carried out for all populations in the batch, and the results are evaluated by a fitness function. The primary target of an HNWS is to meet the grid demand and gain as much as the economic return in the meantime. Therefore, the fitness function is set as a weighted sum of these two aspects, as given by the following equation:

$$score = w_g \Delta grid + w_e \Delta IRR \tag{26}$$

In Eq. (26), w_g and w_e are weighting factors of grid demand and economic gain, respectively. $\Delta grid$ and ΔIRR are the difference of calculated result and target value, which is set by users.

Scores of the batch are compared with the reference score. If the score is better than the reference score, the configuration is kept, otherwise, Russian roulette is performed to decide whether keep the configuration. Selected configurations in this step are named "survivors", and the best score in survivals are recorded.

If the current generation number does not exceed the max generation number, survivors from the last step go through the cross-over and mutation process. In the cross-over process, two configurations are picked randomly from survivals and for each component in the HNWS, a new unit number is achieved by [39]:

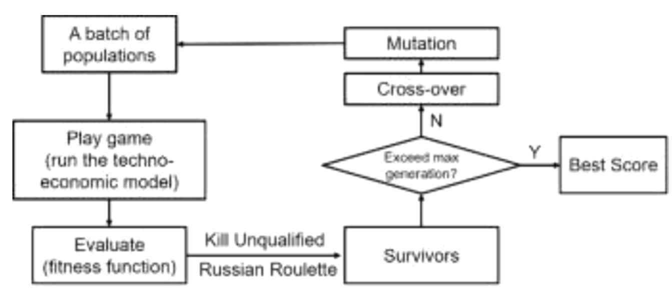

Fig. 8. flowchart of optimization genetic algorithm.

$$int(\xi * n_{p1} + (1 - \xi) * n_{p2}) \tag{27}$$

where ξ is a random number between $[0, 1)$, n is the number of units of the component, and subscript p1 and p2 stands for two configurations.

The mutation is achieved by a user input mutation rate. Each component number in a configuration is converted to a binary number, every digit of the binary may change by the defined mutation rate, and a new configuration is calculated.

With a pre-defined number of generations, an optimized configuration can be achieved that meets the grid demand and gain a better economic return.

4. Results and discussions

In this work, an HNWS is analyzed. As discussed above, the system includes SMRs, wind farms, and PEM stacks. The target of the HNWS is to meet dynamic grid demand data while maximizing system economics.

Table 4
Parameters of components in the HNWS.

	Power (MW)	Lifetime (year)	Construction (year)
SMR	100	60	2
Wind	2.4	30	1
PEM	0.5	20	1

Table 5
Cost data used in the model [32,41–44].

General Economic Data				Wind Cost (Land-base)	
Dollar Base	2018	Discount Rate	5%	Capital Cost ($/kW)	1470
Electricity Price ($/MWh)		$110		OM Cost ($/MWh)	12.1
Hydrogen Price ($/kg)		$8		Decommissioning Cost (MWh)	4.0
Nuclear Costs				**PEM Stack Cost**	
OM Cost ($/MWh)		26.9		Capital Cost ($/kW)	1200
Fuel Cost ($/MWh)		9.3		Operation Cost ($/MWh)	2% of Capital
Decommissioning Cost ($/MWh)		0.16			

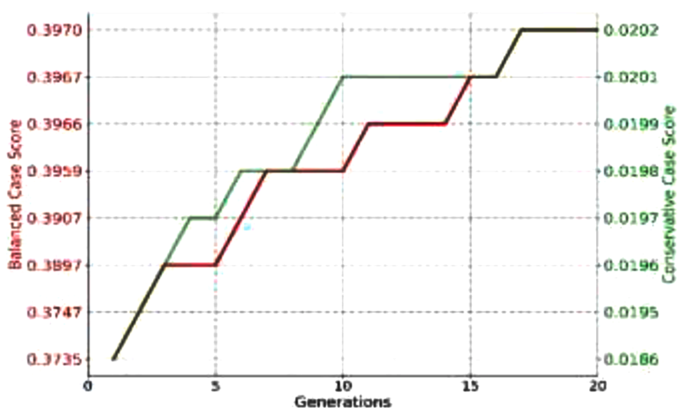

Fig. 9. Scores during generic optimization.

The grid demand data is the UK grid demand data in the year 2018 taken from Grid watch [40]. The data records UK grid demand approximately every five minutes. The HNWS analyzed in this work targets to supply dynamically 2% of real-time UK grid demand. In this work, grid demand data of four typical months, January, April, July, and October, is selected, scaled, and used as input of the model. The scaled grid demand data is plotted in Fig. 8.

Basic parameters of each component like output power, construction time, and lifetime, are listed in Table 4. The output power of wind turbines is typical for land-based wind turbines [41], the output power of PEM cells is achievable with current technology, and the minimum operation power of each PEM cell is set as 0.05 MW. Cost data applied in the model are listed in Table 5, and some detailed technical modeling data can be found in the Appendix. In this work, the 2018 dollar is used. The price of electricity is assumed to be 110 $/MWh [30], which is considered reasonable compared to Hinkley Point C's electricity price [42]. The price of hydrogen is set as 8 $/kg, which is reasonable for current green hydrogen [17,43]. The discount rate is assumed to be 5%. The capital cost of the wind turbine is set as 1470 $/kW [41], and the capital cost of PEM stacks is a median value from the predicted 2020 cost [44] with 2% OM costs.

Different cases are calculated and analyzed: conservative cases, balanced cases, and a nuclear-only case with SMR units of 100 MW_e. Conservative cases are cases that can meet the grid demand as much as possible, while balanced cases are optimized to balance the grid demand and economic return. For analyzes of conservative cases and balanced cases, cases with hydrogen storage and without are conducted, respectively.

While optimizing, the target in Eq. (26) is set to meet 97% of the grid demand for the balanced case, and 100% of grid demand for the conservative case. The economic return target in Eq. (26) is set to be the discount rate. NPPs are considered as FOAK to obtain conservative economic analysis results. In both optimizations, different weighting factors are implemented to Eq. (26). For the conservative case, w_g and w_e is set to be 18.0 and 0.5, while for the balanced case, they are set to be 7.0 and 3.0, respectively. The selection in the conservative case is to make sure the grid fitting plays a dominant role. The optimization is carried out by 20 generations with 20 populations in each generation. In Fig. 9 , maximum scores of each generation are plotted for the conservation case optimization and the balanced case, the optimization achieves an optimized configuration for both cases under the evaluation function.

Table 6
Configurations of different models.

	Conservative	Balanced	Nuclear
SMR Unit	6	4	8
Wind Turbine	150	322	0
PEM Cells	136|0	365|0	0

In Table 6, configurations of optimization results are given. For cases without hydrogen storage, the number of PEMs is set as zero. For comparison, a case of a nuclear system of eight SMR units is analyzed as well.

The grid demand fitting performance of the conservative cases and balanced cases are demonstrated in Fig. 10. These performances are expressed as the differences between grid demand and system supply to grid at a time point, or unfitted demand, in another way of expression. The left figures are the performances of the conservative cases, and the right ones are the balanced cases. In the figure, the upper sub-figures indicate the performances of the HNWS with hydrogen storage while the lower sub-figures are the performances without hydrogen storage. Performances of both cases indicate that the hydrogen storage enhanced the system's overall performance dramatically. Without hydrogen storage, the HNWS can hardly meet the grid demand neither in peak demand month nor normal months in both cases. In the conservative case, the maximum unfitted power reaches over 350 MW frequently in January and around 200 MW in other months without hydrogen storage. This value is as much as about 600 MW in January and 300 MW in other months in the balanced case. The results also demonstrate with hydrogen storage, the conservative model can fully meet the grid demand in all months, while the balanced case can meet the grid demand in most of the cases but not in a few peaks in the peak days in the peak month. The unfitted power condition occurs occasionally only in the worst days of the worst moments in the balanced case, and the unfitted power can be easily fulfilled with the electricity market in these conditions.

Fig. 11 shows the hydrogen storage of the conservative and balanced cases. In both cases, hydrogen storage at the end of each calculated month is larger than zero. For both cases, in the low demand month, the hydrogen production reaches over 30 tons in a month while in the peak demand month the production is low and down to less than 5 tons by the end of the month. In the average month like April and October, the production of hydrogen in both cases is in the range between 20 tons to 25 tons per month.

IRRs and cash flows are analyzed to evaluate the economics of different cases. The cash flows of conservative cases, balanced cases, and nuclear cases are plotted in Fig. 12.The upper figure demonstrates the lifetime cash flow while the lower figure is the cash flow of 20 years since the project started. In the lower figure of Fig. 12, the economics of a reference large reactor with power 1000 MW_e and 7 years construction time is analyzed for comparison. The utilization factor of the large reactor is set to be 0.85. IRRs and LCOEs of these cases (include the

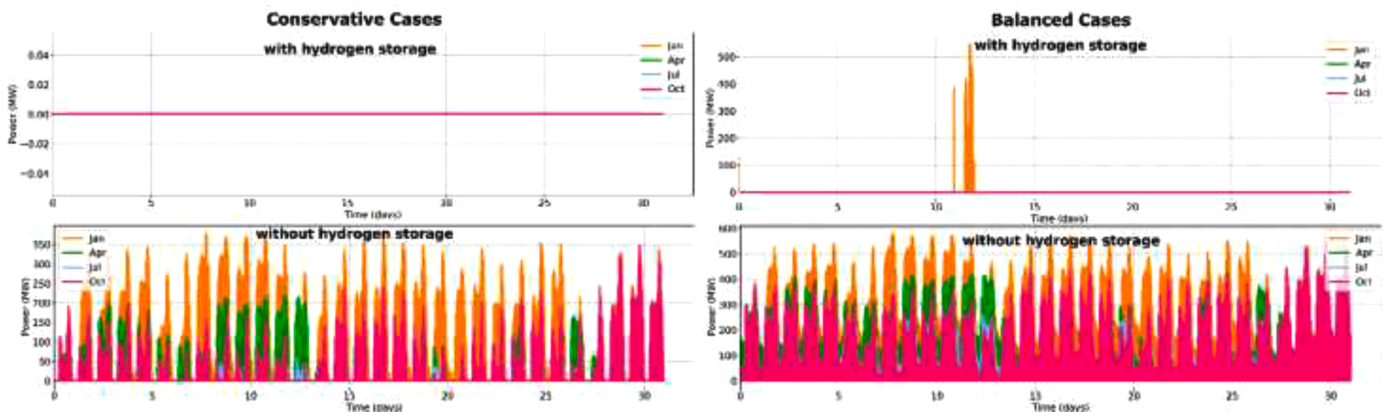

Fig. 10. Unfit grid demand for conservative and balanced cases with or without hydrogen storage (left up: conservative case with hydrogen storage; left down: conservative case without hydrogen storage; right up: balanced case with hydrogen storage; right down: balanced case without hydrogen storage) .

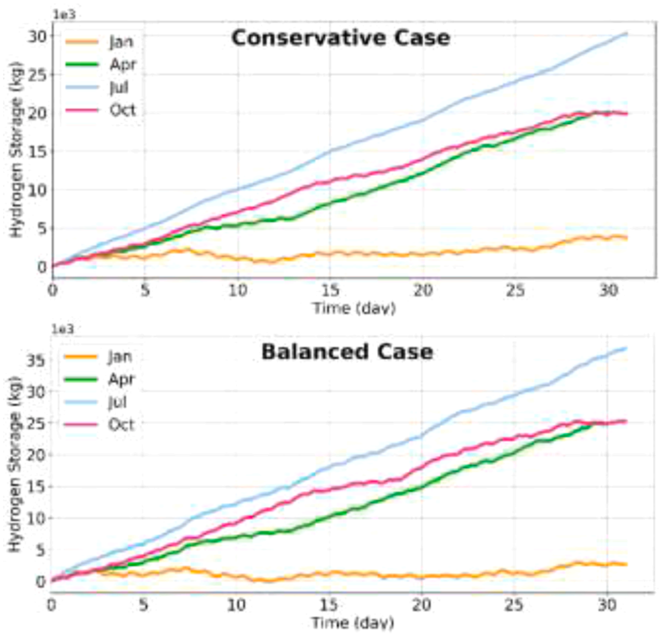

Fig. 11. Hydrogen storage in different months for conservative and balanced cases (upper figure: Conservative case; lower figure: Balanced case, the axial axis value is multplied by 1e3 as marked on the top of the figure).

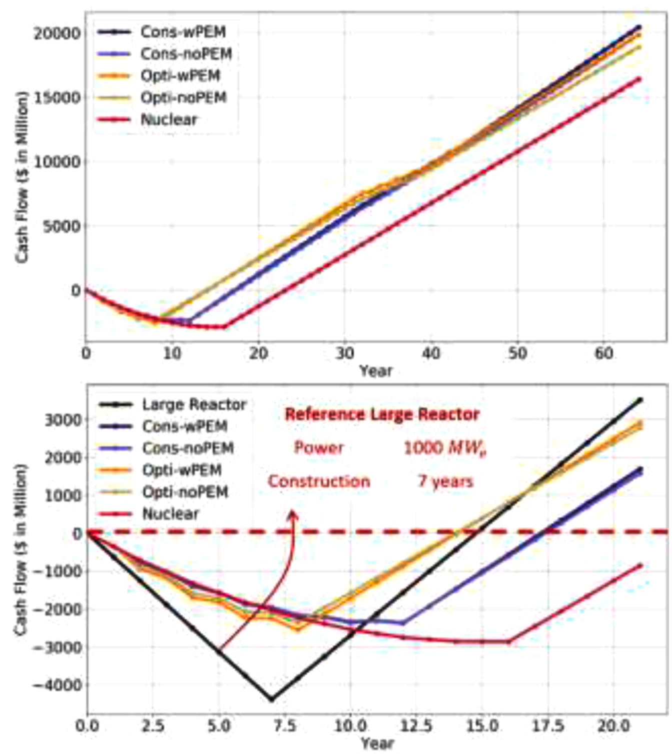

Fig. 12. Cash flow of conservative cases, balanced cases, and SMR units (upper figure: cash flow over the plant lifetime; lower figure: cash flow of 20 years after the first unit starts operating comparing to the reference large reactor).

reference large reactor) are listed in Table 7. In all these cases, the SMR units are also retreated as FOAK to obtain conservative results. The large reactor is considered as NOAK to compare the hybrid system economics to mature technology.

The upper figure of Fig. 12 indicates either with or without hydrogen storage, the hybrid system can obtain a more investor-friendly cash flow. During the construction period, as the lower figure demonstrated, either SMR series or hybrid systems have a flattener cash flow during construction, which will reduce the burden of the vendor. Adding wind farm and hydrogen storage does not increase the cost too much as it can be seen from the comparison between SMR series and balanced cases, yet the balanced hybrid systems have shorter pay-back time. The red line in the lower figure of Fig. 12 is the payback line, it shows from the figure that the reference large reactor normally needs 15 years while with the balanced case, the pay-back time can be one or two years faster. However, the payback time of the conservative cases and SMR series is longer due to the long construction time.

The replacement of wind turbines and PEM units influences the cash

Table 7
IRR and LCOE of different system configurations.

Model	Conservative (with PEM)	Conservative (no PEM)	Balanced (with PEM)	Balanced (no PEM)	SMR Series
IRR	8.91%	9.03%	11.20%	10.33%	6.17%
LCOE	44.71$/MWh	43.79$/MWh	40.24 $/MWh	40.89 $/MWh	53.98 $/MWh

flow. Balanced cases have more wind turbines and PEM units, the upper figure of Fig. 12 shows, by the end of the system lifetime, cash in hand from conservative cases is higher than the balanced cases. Nevertheless, all the hybrid systems obtain a better cash flow than the SMR series all through the lifetime of the project.

As listed in Table 7, the highest IRR in these cases is achieved by the balanced case with hydrogen storage, which reaches up to 11.20%, while without hydrogen storage, the IRR dropped to 10.33% for nearly 1%. The IRRs of the conservative cases are lower, with hydrogen storage, the IRR is 9.03% and without hydrogen storage, the drop is 0.1 to 8.91%. This is due to the contribution of hydrogen storage being less in the conservative case than in the balanced case. Nevertheless, compared to 6.17% of the SMR series, the HNWS can obtain a higher rate of return. For LCOE, the SMR series' cost is calculated as 53.98 $/MWh. The values for conservative cases are 44.71 $/MWh and 43.79 $/MWh, with and without hydrogen storage. Balanced cases obtain even lower values of 40.24 $/MWh and 40.89 $/MWh with and without hydrogen storage. According to these calculation results, the HNWS gains more economic value compared to a single nuclear baseload system, while with hydrogen storage the investment return is even higher.

Fig. 11 also indicates SMR units share a larger fraction of the capital costs. Involving fewer SMR units can increase the economics of the system. Meanwhile, the comparison between conservative case and balanced case shows this may decrease the system stability against grid volatility. However, a proper configuration of wind turbines and PEMs can reduce the gap.

Current models in the HyNuRT code can perform techno-economic analysis of HNWSs. However, there are still limitations. On the technical modeling aspects, the mean and max wind velocity are set to be constant in all months and years, which is not true. Similarly, the grid demand is purely by input without uncertainty in different years. On the economic aspects, the cost of hydrogen storage can transport is not included, neither the cost of dispatching nor related components. Most importantly, the fluctuations of electricity and hydrogen prices on the market are not modeled in the model. In the future electricity market with high renewable penetration, peak-time electricity can be expensive, and add extra-economic gain to an HNWS like the analyzed one. Nevertheless, the current code is capable to capture the mean features of an HNWS with hydrogen storage and give then tendency analysis of the system behavior. In the meantime, uncertainty and sensitivity analyzes are also necessary to increase the credits of the analysis.

5. Conclusion

In this work, techno-economic analyzes are performed for a hybrid nuclear-wind system with hydrogen storage. The open-source HyNuRT code is developed to perform quantitative analyzes of the dynamics of a hybrid nuclear-wind system and the economic value of such a system. The main objective of this method is to obtain insights on whether a hybrid nuclear-wind system with hydrogen storage can fulfill the real-time electricity demand and investment on such systems pay off from basic mechanism level to lifetime system economic analysis. This work also intends to understand how the economic feature of a small modular reactor impacts the system cash flow and investment return.

Analyzes results find that, under proper configuration, a hybrid nuclear-wind system with hydrogen storage can meet the grid demand dynamically in a real grid demand scenario with stochastic wind velocity. By optimization, a conservative configuration can be achieved that can satisfy the grid demand dynamically while keeping the economic gain still better than the SMR series. However, without optimization, there are conditions that hydrogen production is not sufficient, or hydrogen drained out. Meanwhile, hydrogen storage plays a crucial role in system performance. Without hydrogen storage, the electricity demand can hardly be satisfied in all analyzed months in both the conservative case and the balanced case. The peak difference between demand and production can exceed 300 MW in the conservative case and can reach over 500 MW in the balanced case under the worst condition.

Moreover, by the economic analysis based on system performance, the hybrid system shows a higher economic return, a more friendly cash flow as well as a shorter payback time is achieved compared to a pure SMR series. In the conservative scheme, the hybrid system with hydrogen storage increased the internal return rate by 2.74%. In the balanced scheme, the payback time and IRR of the system can be further enhanced by 2.29% compared to the conservative case while losing little on grid demand satisfaction. In both cases, hydrogen storage can increase the economic return by 1% while not strongly impacting the cash flow.

The work also finds out that SMR units share a large fraction of the system cost, fewer SMR units can increase the system economics. However, the reduction of SMR units will decrease system stability against volatility. Proper configuration of the system can reduce this gap while keeping the system run at a high economic condition.

Current models have limitations, too. Constant values of mean wind velocity in different months, grid demand, electricity, and hydrogen prices are considered in the model and cause uncertainties in the results. The optimization process now considers too few parameters. In the future development of the code, the stochastic property of these parameters will be included, and uncertainty and sensitivity studies will be performed. A new wind velocity model according to geographical topology is planned to be included. Different energy storage methods will be implemented and compared. A better optimization methodology will be applied to consider more related parameters and more realized scenarios.

CRediT authorship contribution statement

Tian Zhang: Conceptualization, Methodology, Software, Investigation, Writing – review & editing.

Declaration of Competing Interest

The authors declare that they have no known competing financial interests or personal relationships that could have appeared to influence the work reported in this paper.

Appendix

Technical modeling parameters of wind turbines and PEM units are listed in the following Table A-1.

The economic parameters of nuclear economics are listed in Table A-2. These parameters are applied to the model calculating results in table 5 as well as the HNWS in this work.

Table A-1
Technical modeling parameter of wind turbines and PEM units [24,27,29,41].

Wind Turbine	Wing Diameter	Wind Data	Turbine Working Range	Type
	90 m	Mean 11 m/s Max 28 m/s in 40 ranges	4.0 m/s ~ 25.0 m/s	Land Type Turbine
PEM unit	**Operation Condition**	**Membrane Data**	**Charge Transfer Coefficient**	**Exchange Current Density**
	Temperature 80 °C Pressure 4 bar	Area 120 cm^2 Thickness 0.1 mm	Anode 0.5 Cathode 0.5	Anode 1e-7 A/cm2 Cathode 1e-3 A/cm2

Table A-2
Economic modeling parameter of nuclear [30,32].

Scaling Factor η	x	y	z	k	Learning Rate
0.51	15%	74%	82%	2%	4%

References

[1] IEA, World Energy Outlook 2019, International Energy Agency, Paris, 2019.
[2] IEA, World Energy Outlook 2018, International Energy Agency, Paris, 2018.
[3] Global Energy Transition Statistics, Global Energy Statistical Yearbook 2021, Enerdata, 2021 [Online]. Availablewww.yearbook.enerdata.net/renewables/renewable-in-electricity-production-share.html.
[4] BP p.l.c, BP Energy Outlook 2019 Edition, British Petrol, p.l.c., London, 2019.
[5] IEA, World Energy Outlook 2021, International Energy Agency, Paris, 2021.
[6] B. Zohuri, Hybrid Energy System, Springer International Publishing, 2018, p. 1.
[7] M. Ruth, O. Zinaman, Nuclear-Renewable Hybrid Energy Systems: Opportunities, Interconnections, and Needs, Idaho National Laboratory, 2014.
[8] S. Bragg-Sitton, R. Boardman, M. Ruth, O. Zinaman, C. Forsberg, Rethinking the future grid: integrated nuclear renewable energy systems, in: Proceedings of the 9th Nuclear Plants Current Issues Symposium: Moving Forward, Charlotte, North Carolina, 2014.
[9] D. Mazzeo, N. Matera, P. De Luca, C. Baglivo, P.M. Congedo, G. Oliveti, A literature review and statistical analysis of photovoltaic-wind hybrid renewable system research by considering the most relevant 550 articles: an upgradable matrix literature database, J. Clean. Prod. 295 (2021), 126070.
[10] G. Wang, J. Yin, J. Lin, Z. Chen, P. Hu, Design and economic analysis of a novel hybrid nuclear-solar complementary power system for power generation and desalination, Appl. Therm. Eng. 187 (2021), 116564.
[11] S. Suman, Hybrid nuclear-renewable energy systems: a review, J. Clean. Prod. 181 (2018) 166–177.
[12] R. Pinsky, P. Sabhawall, J. Hartvigsen, J. O'Brien, Comparative review of hydrogen production technologies for nuclear hybrid energy systems, Prog. Nucl. Energy 123 (2020), 103317.
[13] T.E. Baker, A.S. Epiney, C. Rabiti, E. Shittu, Optimal sizing of flexible nuclear hybrid system components considering wind volatility, Appl. Energy 212 (2018) 498–508.
[14] A. Epiney, C. Rabiti, P. Talbot, A. Alfonsi, Economic Analysis of a nuclear hybrid energy system in a stochastic environment including wind turbines in an electricity grid, Appl. Energy 260 (2020), 114227.
[15] M. Ruth, P. Spitsen, R. Boardman, Opportunities and Challenges for Nuclear-Renewable Hybrid Energy System: Preprint, National Renewable Energy Laboratory, Golden, 2018.
[16] M. Ross, H. Bindra, Estimating energy storage size for nuclear-renewable hybrid energy systems using data-driven stochastic emulators, J. Energy Storage 40 (2021), 102787.
[17] D.J. Arent, S.M. Bragg-Sitton, D.C. Miller, T.J. Tarka, J.A. Engel-Cox, R. D. Boardman, P.C. Balash, M.F. Ruth, J. Cox, D.J. Garfield, Multi-input, multi-output hybrid energy systems, Joule 5 (1) (2021) 47–58.
[18] P. Sabharwall, S. Bragg-Sitton, L. Boldon, S. Blumsack, Nuclear renewable energy integration: an economic case study, Electr. J. 28 (8) (2015) 85–95.
[19] IRENA, Hydrogen From Renewable Power: Technology Outlook For the Energy Transition, International Renewable Energy Agency, Abu Dhabi, 2018.
[20] T. Smolinka, Water Electrolysis: Status and Potential for Development. Joint NOW GmbH - FCH JU Water Electrolysis Day, Fraunhofer-Institut für Solare Energiesysteme ISE, Brussels, (BE), 2014.
[21] S. Shiva Kumar, V. Himabindu, Hydrogen production by PEM water electrolysis – a review, Mater. Sci. Energy Technol. 2 (3) (2019) 442–454.
[22] T. Zhang, HyNuRT: hybrid nuclear renewable tool, 2021. [Online]. Available: https://github.com/tzhang0475/HyNuRT.
[23] P. Eberhart, T.S. Chung, A. Haumer, C. Kral, Open source library for the simulation of wind power plants, in: Proceedings of the 11th International Modelica Conference, Versailles, 2015.
[24] IEC 61400-12-1, Wind Turbines - Part 12-1: Power performance Measurements of Electricity Producing Wind Turbines, International Electrotechnical Commission, 2005.
[25] S. Heier, Grid Integration of Wind Energy: Onshore and Offshore Conversion System, 3rd ed., Wiley, Germany, 2014, pp. 438–439.
[26] O. Schmidt, A. Gambhir, I. Staffell, A. Hawkes, J. Nelson, S. Few, Future cost and performance of water electrolysis: an expert elicitation study, Int. J. Hydrog. Energy 42 (52) (2017) 30470–30492.
[27] F. Marangio, M. Santarelli, M. Cali, Theoretical model and experimental analysis of a high pressure PEM water electrolyser for hydrogen production, Int. J. Hydrog. Energy 34 (3) (2009) 1143–1158.
[28] A. Awasthi, K. Scott, S. Basu, Dynamic modeling and simulation of a proton exchange membrane electrolyzer for hydrogen production, Int. J. Hydrog. Energy 36 (22) (2011) 14779–14786.
[29] M. Carmo, D.L. Fritz, J. Mergel, D. Stolten, A comprehensive review on PEM water electrolysis, Int. J. Hydrog. Energy 38 (12) (2013) 4901–4934.
[30] L.M. Boldon, P. Sabharwall, Small Modular Reactor: First-of-a-Kind (FOAK) and Nth-of-a-Kind (NOAK) Economic Analysis, Idaho National Laboratory, Idaho Falls, 2014.
[31] OECD-NEA, Reduction of Capital Costs of Nuclear Power Plants, OECD-NEA, Paris, 2000.
[32] V. Kuznetsov, A. Lokhov, Current Status, Technical Feasibility and Economics of Small Modular Reactors, OECD-NEA, Paris, 2011.
[33] D. Holcomb, F. Peretz, A. Qualls, Advanced High Temperature Reactor System and Economic Analysis, Oak Ridge National Laboratory, Oak Ridge, 2011.
[34] G.A. Black, F. Aydogan, C.L. Koerner, Economic viability of light water small modular nuclear reactors: general methodology and vendor data, Renew. Sustain. Energy Rev. 103 (2019) 248–258.
[35] B. Welsh, Los Angeles Times Data and Graphics Department, A Python Library That Quickly Adjusts U.S. Dollars for Inflation Using the Consumer Price Index (CPI), Los Angeles Time, 2021 [Online]. Available, https://github.com/datadesk/cpi.
[36] M.D. Carelli, P. Garrone, M. Mancini, C. Mycoff, P. Trucco, M.E. Ricotti, Economic features of integral, modular, small-to-medium size reactors, Prog. Nucl. Energy 52 (4) (2010) 403–414.
[37] B. Vegel, J.C. Quinn, Economic evaluation of small modular nuclear reactors and the complications of regulatory fee structures, Energy Policy 104 (2017) 395–403.
[38] NuScale Power, NuScale's affordable SMR technology for all, NuScale Power LLC, Jan. 2020. [Online]. Available: https://www.nuscalepower.com/newsletter/nucleus-spring-2020/featured-topic-cost-competitive.
[39] S. Singh, K.S. Verma, Optimal power flow using genetic algorithm and particle swarm optimization, IOSR J. Eng. 2 (1) (2012) 46–49.
[40] M. Stolworthy, GB electricity national grid demand and output per production type, Grid Watch, 2020. [Online]. Available: https://gridwatch.co.uk/.
[41] T. Stehly, P. Beiter, 2018 Cost of Wind Energy Review, National Renewable Energy Laboratory, Golden, 2018.
[42] BBC, UK Nuclear Power Plant Gets Go-Ahead, BBC co. Ltd, 2013, 21 Oct[Online]. Available, www.bbc.com/news/business-24604218.
[43] J. Eichman, A. Townsend, M. Melaina, Hydrogen Technologies Participating in California Electricity Markets, National Renewable Energy Laboratory, Golden, 2016.
[44] L. Bertuccioli, A. Chan, D. Hart, F. Lehner, B. Madden, E. Standen, Study on Development of Water Electrolysis in the EU. Study on Development of Water Electrolysis in the European Union, Fuel Cells and Hydrogen Joint Undertaking, 2014.